Characterization of novel natural compound derivatives with cancer-selective cytotoxicity

Suneetha Nunna
Leibniz Institute on Aging: Leibniz Institut fur Altersforschung Fritz-Lipmann Institut eV
Ying-Pei Huang
Nuclear Science and Technology development center, national Tsing Hua University, Hsinchu
Mahdi Rasa
Leibniz Institute on Aging: Leibniz Institut fur Altersforschung Fritz-Lipmann Institut eV
Krepelova Anna
Leibniz Institute for Age Research Fritz-Lipmann Institute: Leibniz Institut fur Altersforschung Fritz-Lipmann Institut eV
Francesco Annunziata
Leibniz Institute for Age Research Fritz-Lipmann Institute: Leibniz Institut fur Altersforschung Fritz-Lipmann Institut eV
Lisa Adam
Leibniz Institute for Age Research Fritz-Lipmann Institute: Leibniz Institut fur Altersforschung Fritz-Lipmann Institut eV
Sandra Kaeppel
Leibniz Institute for Age Research Fritz-Lipmann Institute: Leibniz Institut fur Altersforschung Fritz-Lipmann Institut eV
Ming-Hua Hsu
Nuclear science and technology development center, National Tsing Hua University
Francesco Neri (✉ Francesco.neri@leibniz-fli.de)
Leibniz Institute for Age Research Fritz-Lipmann Institute: Leibniz Institut fur Altersforschung Fritz-Lipmann Institut eV https://orcid.org/0000-0003-3903-1974

Research

Keywords: Colorectal cancer, anti-cancer drugs, cancer-selective compounds, natural compound derivatives, colon cancer organoids, Paeonol, α-Mangostin

Posted Date: January 19th, 2021

DOI: https://doi.org/10.21203/rs.3.rs-147861/v1

Abstract

Background

Colorectal cancer (CRC) is one of the most frequent and lethal cancers in the world. The current medical treatment for CRC primarily includes combination of multiple chemotherapeutic, targeted and/or immunotherapeutic drugs. However, these approaches are still not fully successful and cause numerous and severe side effects for the patient. Therefore, there is an urgent need to discover novel and cancer-selective drugs for CRC treatment. As many other natural compounds, a-Mangostin and Paeonol possess anti-cancer properties, but both of these compounds have low solubility and low membrane permeability.

Methods

a-Mangostin and Paeonol derivatives were chemically synthesized to increase cytotoxicity versus cancer cell over non-transformed cells. The anticancer properties of these compounds were investigated on human colon cancer cell lines by employing cell viability, apoptosis and cell-cycle analyses. Transcriptome of cancer cells treated with natural compounds were also analyzed by total RNA-sequencing. Finally, we investigated their effects on human colon organoids derived from healthy and cancerous tissue of the same patient.

Results

We found the two derivative compounds (a-Mangostin-1 (aMan1) and Paeonol-1 (Pae1)) more efficiently induced cytotoxicity in HCT116, HT-29, and SW48 colorectal cancer cell lines than the parental compounds. Both, aMan1 and Pae1 arrested HCT116 cells in G1 and HT-29 and SW48 cells in G2/M phase of the cell cycle. aMan1 and Pae1 induced selective transcriptional responses in CRC cells involving genes related to metabolic stress and DNA damage response signaling pathways. Both aMan1 and Pae1 induced apoptosis in human cancer cells and organoids derived from tumor tissue without affecting the viability of human non-cancer cells and intestinal organoids derived from healthy tissue.

Conclusions

Our findings increase the knowledge about natural compound derivatives as anticancer compounds and open new research options on the derivation of lead compounds aimed to the development of novel CRC chemotherapeutic drugs that selectively target cancer, but not healthy cells.

Background

Colorectal cancer (CRC) is the third most prevalent cancer in the world a malignancy that is frequently caused by life style, diet, and genetics [1, 2]. CRC is also an age-related disease with increasing incidence rate with aging, especially after the age of 50. Currently, CRC has a very differential prognosis. At the early stage of diagnosis, the five-year survival rate of the patient is 90%. However, if diagnosed at a metastases stage, the five-year survival rate drops to 10% [3]. The current medical CRC treatments usually include a

combination of multiple chemotherapeutic, targeted and/or immunotherapeutic drugs [4, 5]. However, such therapies are often still inefficient to completely cure CRC and have numerous and severe side effects on the patients health. The side effects of drug-mediated therapies depend on the type, dose and duration of the treatment and are usually caused by the lack of a drug's cancer-specificity. Due to these severe side effects, chemotherapy is often designed taking in consideration the health status of the patient and the medical history. In recent years, a large effort has been devoted to provide psychological and medical support to patients dealing with severe side effects [6-8]. In summary, the high morbidity and mortality associated with CRC and the inefficacy of the current available drugs to selectively target cancer cells increases the demand to find novel cost-effective anti-cancer agents.

Natural compounds have emerged as economic, practicable and effective therapeutic approaches for treatment of cancer. Natural compounds (phytochemicals) are substances with potentially bioactive properties produced by microbes or plants. Phytochemicals have been largely shown to suppress carcinogenesis *in vitro* studies and in pre-clinical models. Almost half of the approved chemotherapeutic drugs are derived from natural compounds or their derivatives [9-12]. One class of chemical natural phenolic compounds, the Xanthonoids, have shown potential anti-cancer, anti-inflammatory, and anti-oxidative properties [13, 14] Among xanthonoids, the compound a-Mangostin derived from *G. mangostana* has been shown to have a broad functional activity. For example, a-Mangostin induces a variety of pharmacological functions: anti-oxidant, anti-carcinogenic, and anti-diabetic. Among them, the anti-cancer activity is the most promising [15]. a-Mangostin affects the growth of the tumor cells *in vitro* and *in vivo* including in high-grade malignancies. a-Mangostin inhibits the migration and invasion, and it reduces the actin cytoskeleton of human lung cancer cells, thereby it exhibits anti-metastatic activities [16]. a-Mangostin inhibits the activation of TAK1–NF-κB pathway, thus acting as an anti-inflammatory compound [17]. It also induces mitochondrial dysfunction [18]. Furthermore, it induces apoptosis and cell cycle arrest in human colon cancer cell lines DLD-1, HCT116 and HT-29 [19] and blocks tumor growth in mouse xenograft models [20].

Another class of natural phenolic compound Paeonol (2-hydroxy-4-methoxyacetophenone) is a bioactive component isolated from the root bark of *P. suffruticosa Andr* [21-23]. Paeonol has been widely used as an anti-inflammatory drug for repairing oxidative damage and enhancing immunity function. It also reduces the severity of liver fibrosis and prevents ox-LDL-induced endothelial cell apoptosis [24]. Paeonol inhibits the growth of colorectal cancer cell lines HCT116, SW620, and it down regulates the expression of COX-2 and PGE2 synthesis in colorectal cancer LoVo cells [25]. Paeonol significantly lowers the tumor growth and causees tumor regression in a gastric cancer cell line MFC tumor-bearing mice [22].

Despite the broad functional activity of a-Mangostin and Paeonol, both of these compounds have an intrinsically low solubility and low membrane permeability that are chemical properties that made them fail to reach clinical applications. We speculate that an enhanced solubility, improved cell membrane penetration and/or by adding new functional groups may potentiate their anti-cancer activity and selectivity as well as increase their therapeutic potential.

This study aimed to improve the cancer cytotoxicity and selectivity of a-Mangostin and Paeonol by addition of new functional groups. As the cytotoxicity of parental compounds have been tested on colon cancer cell lines and our lab is mainly focused on colon cancer, we investigated the effect of two very promising a-Mangostin and Paeonol derivatives against human colon cancer cell lines and human intestinal organoids. We found that the two derivatives showed a much lower toxic effect on not transformed human cells with respect to their parental compounds. Our findings increase the knowledge about natural compounds derivatives as anticancer compounds and open new research options on the derivation of lead compounds such as novel CRC chemotherapeutic drugs that selectively target cancer, but not healthy cells.

Methods

Cell viability assay

BjhTERT (RRID_CVCL_6573), HCT116 (ATCC, CCL-247), HT-29 (ATCC, HTB-38) or SW48 (ATCC, CCL-231) cells were cultured in RPMI (GIBCO) supplemented with 10% FCS, 1mM sodium pyruvate and 1X glutamax. To determine the effect of natural compounds on cell viability, the above-mentioned cell lines 5000 cells/ well were seeded in a 96-well plate. The next day, cells were treated with different concentrations of either aMan (5, 10, 25, and 40 µM) or aMan1 (5, 10, 25, and 40 µM), Pae (100, 200, 300, and 400 µM), or Pae1 derivatives. After 72 hours of incubation, the cell supernatant was removed, and the adherent cells were fixed with paraformaldehyde (4%) for 15 minutes and stained with 50 µl of crystal violet blue (0.1 %) for 30 minutes on an orbital shaker at room temperature. Then, the cells were washed twice with 200 µl of autoclaved distilled water, and the dye was dissolved in 100 µl of acetic acid (10%). The dissolved dye was transferred to flat bottom 96-well plates for measuring the absorbance at 570 nm.

Apoptosis analysis by flow cytometry

The cells BjhTERT, HCT116, HCT116 TP53_KO, HT-29 or SW48 cells ($1X10^5$ cells/ well) were seeded on a six-well plate. Then, the cells were incubated either with aMan (25 µM), aMan1 (25 µM), Pae (300 µM), or Pae1 (10 µM) for 48 h. After incubation, the adherent cells were trypsinized and harvested including the floating cells in culture medium. The cells were washed once with PBS and incubated in 100 µl of 1X Annexin V binding buffer for 20 minutes on ice. After washing, the cells were resuspended in PBS with 0.1% FBS containing DAPI and analyzed by flow cytometry with FACScanto™.

DNA Fragmentation assay

SW48 cells ($1X10^5$ cells/ well) were seeded in a six-well plate, and the cells were treated with aMan1 (25 µM) or Pae1 (10 µM) for 72 hrs. After incubation, the adherent as well as floating cells were harvested and genomic DNA was isolated with the use of DNeasy blood and tissue kit (Qiagen). Genomic DNA (2 µg) was incubated with 2 µl of RNase cocktail. The genomic DNA of (1 µg) was resolved on 2% Agarose gel containing ethidium bromide. The image was acquired using Gel Doc (Bio-Rad).

Confocal Microscopy

SW48 cells (1X10^5 cells/ well) were cultured in a six-well plate on glass cover slips in RPMI medium supplemented with FCS (10%). Then the cells were treated with aMan1 (25 µM) or Pae1 (10 µM) for 72 hrs. Followed by incubation, the cells were fixed with paraformaldehyde (4%) and permeabilized with triton X100 (0.2 %) in PBS for 10 minutes. After washing with PBS, the cells were blocked with 5 % skim milk powder overnight and the nuclei were stained with DAPI for 1 h hour at room temperature. After three washes with PBS, the slides were mounted on glass slides using DPX mounting medium and cured for overnight. The images were captured using a Zeiss Apotome.

Cell cycle analysis

To investigate the effect of natural compounds on cell cycle, BjhTERT, HCT116, HT-29, or SW48 cells (1X10^5 cells/well) were seeded in 96-well plates and treated with either aMan (25 mM), aMan1 (25 mM) Pae (300 mM) or Pae1 (10 mM) for 48 h. Then the cells were incubated with EdU (10µM) for 20 min. After trypsinization, the cells were harvested, fixed with paraformaldehyde (4%) at room temperature for 15 minutes and permeabilized with Triton X100 (0.25 %) for 10 minutes. Then the incorporated EdU was stained according to the manufactures protocol. After staining the cells with DAPI, the cells were analyzed by FACScanto™.

Western blotting

HCT116 WT and KO cells were harvested and washed with 1X PBS twice and cells were lysed in RIPA buffer (50 mM Tris-HCl pH 8.0, 150 mM NaCl, 1% NP-40, 0.5% DOC, 0.1% SDS. Then the cells with RIPA buffer were incubated on ice for 15 min, and sonicated using the Bioruptor Next Gen (Diagenode) for 5 cycles (30 sec on and 30 sec off) at high power setting. After centrifugation at 20.000xg for 15 min at 4°C, the supernatant was collected and the total protein was quantified using Pierce™ BCA Protein Assay Kit (Thermo Fisher Scientific). The protein extracts were run on 4–20% Mini-PROTEAN TGX Stain-Free Gels (Bio-Rad), and transferred to nitrocellulose membranes (iBlot® 2 Transfer Stacks; Thermo Fisher Scientific). After the transfer the membranes were blocked in T-PBS (0.1% Tween 20 in PBS) supplemented with 5% milk for 2 hours at RT, and then incubated with p53 WT specific antibody (Sigma, A5316) and Beta actin (Santa Cruz, sc126) mouse antibodies in T-PBS + 5% BSA overnight at 4°C. After incubation with primary antibody, the membranes were washed six times with T-PBS for 30 min at RT, and then incubated with secondary anti moue HRPO antibody (1:3000) in T-PBS + 5% milk for 1 hour at RT. After incubation with secondary antibody, the membranes were washed six times with T-PBS for 30 min at RT, and then developed on Amersham Imager 600 (GE Healthcare).

Human intestinal crypt isolation and cultivation

Human intestinal crypts were isolated from either tumor tissue or adjacent healthy tissue from the same patient and cultured to intestinal organoids as previously shown [33].

Live and dead organoid quantification

Human intestinal organoids were seeded (100/ well) in Labtec (Eschelbronn, Germany) chamber slides containing 20 µl of matrigel matrix and 300µl of growth medium. After 24h of culturing, organoids were treated with various concentrations of either Irinotecan (3, 6, and, 12 µM) aMan (25, 50, and 100 µM), aMan1 (25, 50, and 100 µM), Pae (100, 200, and 400 µM), or Pae1 (7.5, 15, and 30 µM) for additional 48h. Then the images of organoid were captured with the use of Zeiss AxioCam MRc 5 (Carl Zeiss). Live and dead organoids were enumerated by their morphological appearance as described [34].

Quantification of organoids cell death by flow cytometry

Human intestinal organoids were seeded and treated with different concentrations of either irinotecan, aMan, aMan1, Pae or Pae1. Following 48 h of incubation, the organoids were harvested, washed with 1X PBS, and incubated with 200 µl of TrypleE mix (1M MgCl2, 10mM Y27, 0.5M EDTA, 1MCacl2 and 5µl DNAsel) for 10 min at 37 ^{O}C. The organoids were made into single cell suspensions by vigorous pipetting 40-50 times. The cells were washed and resuspended in FACS buffer containing 2% FCS and 100 µM of LY27632. The samples were analysed using FACScanto™ (BD bioscience).

RNA sequencing library preparation and data analysis

For RNAseq analysis, BjhTERT, SW48, HCT116_TP53_WT, and HCT116_TP53_knockout (KO) cells were cultured in RPMI (GIBCO) medium supplemented with 10% FCS, 1mM Sodium pyruvate (GIBCO) and 1X Glutamax (GIBCO). These cell lines (1 × 10^5cells/ well) were seeded in a 6-well plate. The next day, cells were treated with either aMan1 (25 µM) or Pae1 (10 µM) 42 h. Total RNA was isolated with the use of QIAzol Lysis (Qiagen) followed by isopropanol precipitation. Then, concentration and integrity of RNA was estimated with the use of Fragment Analyzer (Agilent) and Qubit 4 Fluorometer (Thermo Fisher). Poly-A tail mRNA was enriched using magnetic beads. The first strand of cDNA was synthesized using Superscript III Reverse Transcriptase (Thermo Fisher), and the second strand was synthesized using the second strand master mix (TruSeq RNA Library Prep Kit V2 (Illumina)). The synthesized DNA was cleaned up with the use of AgencourtAMPure XP Beads (Beckman Coulter). After, end repair/dA-tailing, adaptors were ligated, and the library was further enriched with the use of TruSeq RNA Library Prep Kit V2 (Illumina). After determining the quality and concentration, the cDNA libraries were pooled and loaded (20 pM) into the NextSeq 500 (Illumina) Sequencer with the use of NextSeq 500/550 High Output Kit v2.5(75 cycles).

Fastq files quality check was performed using FastQC v0.11.5. The fastq files were mapped to the hg19 genome using TopHat v2.1.0 [35] with the following parameters –bowtie1 –no-coverage-search -a 5. The number of reads covered by each gene is calculated by HTSeq-Count 0.11.2 [36] with -s no -a 0 -t exon -m intersection-nonempty parameters and hg19 gencode.v19 annotation. Before further analysis, all of the rRNA genes are removed from the count data. For calculating differentially expressed genes and normalized count, DESeq2 R package v1.20.0 [37] was used with the default parameters. For Pearson correlation analysis, principal component analysis (PCA), gene set enrichment analysis (GSEA) and

plotting the expression, the normalized count (DESeq2) was used. For PCA and Pearson correlation, only the genes with more than 10 counts in at least 3 samples and with the minimum inter quadrille range (IQR) of 1.5 in log2 transformed normalized counts were used for calculation. For functional and pathway analysis, DESeq2 differentially expression analysis (adjusted p-value<0.01 & | log2 fold change | >=1) results were uploaded in IPA (Ingenuity Pathway Analysis v45868156 [38].

For gene set enrichment analysis, normalized counts (for each gene in all of the samples) were scaled using scale function in R (with center = TRUE, scale = TRUE parameters). The z-score was calculated by multiplying the scaled counts by +1 or -1 which shows the expected direction (+1 for up-regulated genes and -1 for down-regulated genes). For figure 5F and 6F, +1 is used for all of the genes in the 3 gene sets (same genes as figure 5E) except CDKN2B which -1 is used. For the canonical pathways in figure S4C and S5A, the gene list and the directions are extracted from DEGs (adjusted p-value<0.01 & | log2 fold change | >=1) in comparison between SW48 cells treated with aMan1 versus DMSO, and for figure S4D and S5B, DEGs from the comparison between SW48 cells treated with Pae1 versus DMSO is used. The average of z-scores were calculated for each group (one value for each gene per group) and used for plotting and statistical test.

Statistical Analysis

The statistical significance between two groups were analysed by two-tail unpaired T-test followed by Holm-Sidak correction for multiple comparison using Graphpad Prism 5 (GraphPad Inc., La Jolla, CA, USA). Differences with $p < 0.05$ were considered significant, and statistical significance is shown as $*p < 0.05$, $**p < 0.01$, $***p < 0.001$.

Results

Cell viability screening of a-Mangostin, Paeonol, and their derivatives in CRC cell lines.

aMan1 with an aldehyde group was prepared to leave the xanthone core intact, to improve solubility and to reduce the cytotoxicity. Although Paeonol exhibits good anti-inflammatory/ oxidative activity and low cytotoxicity, it barely showed an anti-cancer effect. Moreover, its low solubility reduced its usefullness. To increase the solubility with facile synthesis, the boronic acid group was used. More importantly, when attached to a sugar (ex: a fructose), the boronic acid-fructose group can increase the selectivity of a compound concerning tumor cells. This idea is based on the design concept of boronophenylalanine-fructose (BPA-fructose), an agent applied in a clinical trial of boron neutron capture therapy. Even without the attachment of a sugar moiety, the strong affinity of a boronic acid group to the cell membrane can enhance the bioactivity of a compound that has interactions on membrane proteins expressed more on tumor cells. In brief, we tried using a boronic acid group to improve solubility and, once needed, to attach a sugar moiety for “indirectly” increasing the selectivity over tumor cells. The overall cytotoxicity of Paeonol will be increased when transformed into a chalcone, but the selectivity over tumor cells became greater due to a boronic acid group allowing lower dosages.

We performed a medium-throughput screening of all the derivatives on HCT116, HT-29 and SW48 colon cancer cell lines to test whether these derivatives have an enhanced activity in selectively inhibiting cancer cell growth (Figure 2 and S2). Indeed, we could identify two derivates: 2-(3,6,8-trihydroxy-2-methoxy-7-(3-methylbut-2-en-1-yl)-9-oxo-9H-xanthen-1-yl) acetaldehyde that we named α-Mangostin-1 (aMan1) and (E)-(4-(3-(2-hydroxy-4-methoxyphenyl)-3-oxoprop-1-en-1-yl)phenyl) boronic acid that we named Paeonol-1 (Pae1) (Figure 1), which exhibited enhanced antiproliferative properties towards colon cancer cell lines compared to non-transformed cells (human non-cancerous fibroblasts, BjhTERT). The parental compound α-Mangostin (aMan) used at 40 μM totally reduced the viability of HCT116, and HT-29 colon cancer cells by 100% and SW48 cells by 92% (Figure 2a), but also of human non-cancerous fibroblasts (BjhTERT). The derivative compound aMan1 (at 40 μM) decreased the viability all of the three-colon cancer cells by 95-99%; however, it was less toxic towards the human non-cancerous fibroblasts (BjhTERT) and reduced the viability by only 30% (Figure 2b). Thus aMan1 showed to more specifically target colon cancer cells and to less affect the viability of non-cancerous fibroblasts.

Pae showed cytotoxic effects on cancer cell lines, but required a high concentration (300 μM) to reduce the viability of HCT116, HT-29, and SW48 cells by ~90% (Figure 2c). Pae1 required a consistently lower concentration (25 μM) to reduce the viability of HCT116, HT-29, and SW48 to 91%, 75%, and 86%, respectively (Figure 2d) and showed a higher cancer cell specificity compared to the parental compound. The other Pae derivatives showed no evident higher cancer-specific cytotoxicity than the parental compound (Figure S2a, b, and c). Therefore, Pae1 displays more effectiveness at a low concentration and more selectivity than the parental compound against human colon cancer cell lines.

Characterization of the cytotoxic property of a-Mangostin, Paeonol, and their two enhanced derivatives in CRC cell lines

To better characterize the reduced viability of the CRC cell lines, we performed a flow cytometry (FACS) analysis with DAPI and Annexin V staining. DAPI reveals cell membrane permeability therefore is an indicator of cellular death and Annexin V is a marker for apoptotic cells (Figure 3 and S3). Both, aMan and aMan1 induced cell death in all cancer cells used in the experiments (Figure 3a). However, aMan1 induced significantly higher percentages of cell death in the cancer cell lines with respect to the parental compound (Figure 3b - top panel). aMan1 also showed strongly significant reduction of cellular death in BjhTERT cells when compared to the aMan treatment (Figure 3b - top panel). Similarly, Pae used at high concentrations (300 μM) induced cell death of CRC cells (Figure S3a, quantification in Figure 3b – bottom panel). However, Pae1 required a much lower concentration (25 μM) to induce significantly higher cell death in colon cancer cells, yet maintaining less toxicity properties against BjhTERT cells with respect to Pae (Figure 3b - bottom panel).

To further understand whether the cellular death was mediated by an apoptotic program, we performed FACS analysis with Annexin V staining (Figure 3c, d and S3b). In all of the three CRC cell lines the derivative compounds showed a significantly higher induction of apoptosis, while no apoptosis was observed in the BjhTERT cells (Figure 3c, d and S3b). Pae1 also allowed us to use a lower concentration

compared to its parental compound (Figure d, bottom panel and S3b). Analysis of DNA fragmentation by agarose gel and DAPI fluorescence imaging confirmed the induction of apoptosis following aMan1 and Pae1 treatment (Figure 3e, and f). Thus, aMan1 and Pae1 displayed a significantly higher apoptosis-inducing activity in CRC cells, but not in non-transformed cells.

Characterization of the effect of a-Mangostin, Paeonol, and their two enhanced derivatives on the cell cycle in CRC cell lines.

As an apoptotic program may be induced by the arrest at specific cell cycle phases, we analyzed the cell cycle status by flow cytometry (Figure 4). Both aMan and aMan1 arrested HCT116 cell lines in G1 phase of cell cycle (Figure 4a, quantification in b). Interestingly, these two compounds arrested HT-29 and SW48 cell lines in the in G2/M phase of cell cycle (Figure 4a, and b). However, we also observed, especially in HT-29 and SW48 cells, an increase of the overall DNA content indicating a potential appearance of polyploid cells perhaps due to events of endoreduplication suggesting that these two compounds may arrest cells in G2/M phase or rather increase the number of polyploid ($\geq$4n) cells in an aberrant G1 phase. Similarly, Paeonol and Paeonol-1 arrested HCT116 cell lines in G1 phase of cell cycle and HT-29 and SW48 cell lines in the G2/M (or G1 phase of polyploid cells) phase of cell cycle (Figure 4c, quantification in d). These results indicate that the derivative compounds arrest the cell cycle of colon cancer lines in a similar (slightly more powerful) manner with respect to their parental compounds suggesting similar mechanisms of action and that the response to the treatment can be different in different CRC cells.

Characterization of the transcriptional response following of a-Mangostin-1 and Paeonol-1 treatment in SW48 CRC cell line.

To better characterize the molecular phenotype, we performed transcriptomic analysis (RNA-seq) of the SW48 cells treated with aMan1 or Pae1 for 24 hours. Hierarchical clustering heat-map of Pearson correlation of whole-transcriptomes showed that the Pae1 or aMan1 treated SW48 cells clustered separately with respect to the untreated cells (2 replicates for each condition), in contrast to the treated and untreated BjhTERT cells which clustered together (Figure 5a and b). PCA analysis of the datasets further confirmed that BjhTERT were not transcriptionally affected by aMan1 treatment and slightly responded to the Pae1 treatment (Figure S4a, and b). These two analyses highlight the fact that the Pae1 or aMan1 treatments induced a more massive transcriptional response in cancer cells than in non-transformed cells. The finding is confirmed by the number of significantly differentially expressed genes (DEGs) following treatments that was about ten times higher in SW48 cells than in BjhTERTcells (Figure 5b).

We performed Gene Ontology (GO) analysis of the DEGs in cancer cells and we found that both aMan1 and Pae1 treatments induced transcriptional regulation of genes involved in cell cycle regulation and DNA damage response confirming the results of the experiments described in figure 3 and 4 (Figure 5c and d). In particular, proliferation-associated genes (e.g. CCND1, CCNA2, PCNA) were strongly downregulated, while cell cycle inhibitors like CDKN2B is upregulated in cancer cells after treatments (Figure 5e and f - left panel). Pae1, but not aMan1 slightly affected these genes also in the BjhTERT

(Figure 5e and f - left panel). Remarkably, cancer cells treated with both the compounds showed a strong upregulation of genes involved in DNA damage response and in the EGR/NF-kB pathways (Figure 5e and f – middle and right panels) suggesting that NF-kB, EGR and GADD45 genes may be sequentially activated upon DNA damage following treatment with the compounds [29]. Interestingly this pathway is only activated in cancer, but not BjhTERT cells. GO analysis also showed enrichment of signaling pathways involving genes that might be regulated in metabolic stress response. In particular EI2F signaling, mTOR signaling and protein ubiquitination pathways may indicate an endoplasmic reticulum (ER) stress in cells treated with aMan1, while oxidative phosphorylation, sirtuin signaling and mitochondrial dysfunction pathways suggest the occurrence of a mitochondrial stress response in cells treated with Pae1 (Figure 5c and d). Geneset enrichment analysis of these pathways showed that ER stress response related genes were specifically enriched only in SW48 cells after aMan1 treatment, while mitochondria stress response associated pathways were specifically enriched in cancer cells treated with Pae1 (Figure S4c, and d).

Cytotoxic activity of a-Mangostin-1 and Paeonol-1 and cellular stress response following treatment is largely maintained in TP53 deficient CRC cells.

Since we found enrichment of the P53 signaling pathway (Figure 5c and d) and it has been previously reported that aMan induces apoptosis in a P53 dependent manner [11], we questioned if the P53 proficiency was a necessary condition to preserve the cytotoxicity and cancer selectivity of the two derivative compounds. Therefore, we tested the aMan1 and Pae1 on HCT116 cells having wild type (WT) or mutant (inactive) p53. Cells with mutant p53 showed a decreased apoptosis following aMan1 and Pae1 treatment (from ~41% to ~33% and ~44 to ~27%, respectively) suggesting that p53 is indeed important in inducing aMan1-mediated apoptosis, but also that additional p53-independent pathways are taking place to carry out this function (Figure 6a and b). RNAseq analysis of the HCT116 cells treated with aMan1 and Pae1 showed that, even though transcriptionally different, HCT116 WT or KO for TP53 responded similarly to the two derivative compounds (Figure 6c). TP53-WT HCT116 cells have a higher basal expression of the TP53 gene and its known targest P21 and $P15^{INK4b}$ [30] as well as transcriptional upregulation of these genes in contrast to the TP53-KO HCT116 cells (Figure 6e). However, both the HCT116 cell lines have a downregulation of cell-cycle related genes, and upregulation of genes belonging to DNA damage and EGR/NF-kB signaling pathways as previously observed in the SW48 CRC cell line (Figure 6f). Remarkably, ER-stress response pathways were again observed only following aMan1 treatment (in both TP53-WT and TP53-KO HCT116 cells) (Figure S5a). Mitochondrial stress response pathways were observed in both the cell lines and following the treatments with both aMan1 and Pae1 (Figure S5b).

These results suggest that aMan1 or Pae1 may induce a cellular metabolic stress involving ER or mitochondria that can lead to DNA damage and activation of both TP53-dependent and -independent cell-cycle arrest and induction of the apoptotic programs. One candidate pathway involved in the DNA damage response is the NF-kB/EGR/GADD45 pathways that has already been demonstrated to work in a TP53-independent manner [31]. Very importantly, neither the metabolic stress nor the potential

consequent DNA damage and DNA damage response is shown in non-cancer BjhTERT cells. These analyses revealed the importance of the cancer mutational profile in modulating the anticancer activity of the aMan1 and Pae1 treatment, but also provide evidence that these compound derivatives may be also used in P53-deficient tumors.

Taken together these results show that aMan1 and Pae1 provoke a strong transcriptional response in CRC cells (not present in non-transformed cells), involving metabolic stress and DNA damage response signaling pathways, ultimately leading to cell cycle arrest and induction of apoptotic programs.

Characterization of the cytotoxic property of a-Mangostin, Paeonol, and their two derivatives in human primary intestinal organoids

To investigate the effect of natural compounds on human intestinal organoids, we have isolated the crypts from colorectal tumor tissue as well as normal colonic epithelium from samples (surgery leftover) of the same patient. This procedure allows culturing the organoids side-by-side and testing and screening of drugs for their anticancer activity, and assessing the adverse toxic side effects on normal tissue. To assess whether natural compounds induce apoptosis selectively in tumor cells, human colon cancer organoids and healthy tissue organoids from the same patient were plated in equal number, and organoids were treated with various concentrations of aMan, aMan1, Pae or Pae1 for 48 h (Figure 7a). We used irinotecan (a camptothecin (CPT) analog) that is currently used as chemotherapeutic drug for CRCs and DMSO as a negative control. At the minimal concentration required to induce cellular death in all of the cancer organoids, irinotecan, aMan and Pae were also inducing cellular death in ~50% of the colon organoids derived from the cancer surrounding healthy tissue (Figure 7a, quantification in b). Importantly and reflecting the cell viability assays in the CRC cell lines, aMan1 and Pae1 did not show any cytotoxic effect in the healthy colon tissue cultures (Figure 7a, quantification in b). Furthermore, the cell death induced by the natural compound was analysed with the use of flow cytometry (Figure S6). irinotecan, Man and Pae compounds induced cell death in cancer organoids and also healthy colon organoids. However, Man1 and Pae1 induced cell death only in cancer organoids without inducing any cytotoxicity in healthy organoids (Figure S6).

In cancer organoids, aMan1 and Pae1 induced apoptosis (Figure 7c and d), but no apoptosis was observed in healthy organoids. Therefore, aMan1 and Pae1 showed a higher induction of cell death and apoptosis in cancer organoids but not in healthy organoids.

Taken together these results confirm that our observations from the 2D CRC cell lines are also applicable in ex-vivo human organoids, strongly suggesting that the two derivatives of the natural compounds α-Mangostin and Paeonol have a strong selectivity in targeting only cancer cells and promoting them as potential novel promising compounds for the treatment of CRC patients.

Discussion

CRC is one the most frequent cancers in both men and women in the world. According to the American Cancer Society, this cancer is the cause of ~50 thousand deaths per year in the USA. Patients with metastatic CRC that are usually treated with multiple therapeutic lines involving potent chemotherapeutic drug cocktails have a higher mortality risk [32]. Most of these drugs have very severe adverse effects and, often, the therapy has to be designed in according to the medical history and the health condition of the patients. In many cases chemotherapy initially works; however, there is often problems of dosage, relapse, and adverse effects indicating an urgent need for more novel treatment options. Therefore, the development of novel chemotherapeutic drugs that selectively kills the tumor cells, leaving the healthy cells alive could provide a potential way for treating CRC. In the last years, many attempts (sometimes successful) have been done to develop more powerful cancer specific drugs and to reduce the side effects of the treatment. For example, the development of molecular-targeted agents and immunotherapies that are targeting specific molecules expressed only, or more abundantly, in the tumor cells. Drug development and testing for CRC is continuously evolving (e.g. in USA there currently are more than 50 different clinical trials in more than 1000 locations) and the promise of cancer-specific therapeutic treatments still remains an unmet medical priority [32].

Natural compounds represent a wide variety of relatively cheap and suitable molecules that often have been used for various therapeutic aims since ancient times; for example, a-Mangostin and Paeonol derived from plants are used in the traditional Chinese medicine. However, these two compounds, although they showed mild anti-cancer properties, never reached a clinical phase because of some physical and chemical features (e.g. low solubility and low membrane permeability) that make them unsuitable as drugs. In this study, we tested some chemical derivatives of these two compounds aimed to enhance their solubility, cell membrane penetration and/or cancer selectivity. We screened for those derivatives that performed better than the parental compounds, with particular focus on two important features (enhanced cytotoxicity and cancer selectivity) and two of them (named aMan1 and Pae1) were selected for further characterization. FACS analysis of the cell viability, cell death and apoptosis as well as transcriptome profiling confirmed that these two derivatives have enhanced cytotoxicity and cancer-cell selectivity. RNA-seq analysis indicated that the two compounds might cause metabolic stress in the cells (probably by inducing ER or mitochondria stress) and to further activate the DNA damage response that leads to cell cycle arrest and apoptosis of cancer cells. We also showed that aMan1 and Pae1 have similar activity (slightly lower) in cancer cell lines deficient for TP53, one of the major players in mediating cell apoptosis probably through the P53-independent signalling of the NF-kB/EGR/GADD45 pathway [31]. Finally, we showed that aMan1 and Pae1 are able to kill organoids from colon cancer, and do not show any toxic effect on colon organoids from healthy tissue. Therefore, they performed much better than the parental compounds as well as some currently used chemotherapeutic drugs like irinotecan.

Conclusions

In this study, we have screened a series of natural compound derivatives to find those that improved toxicity against cancer cells with respect to the parental compounds and to currently used

chemotherapeutic drugs for the CRC treatment (like Irinotecan). Our data revealed two natural compound derivatives (named aMan1 and Pae1) high cancer-selectivity and cytotoxic activity. Cell viability assays, FACS analysis and transcriptome analysis confirmed that these two compounds induce cell death and apoptosis in CRC cell lines and in organoid derived from human colon tumors, but not in non-cancer human cells and in organoids derived from healthy colonic epithelium. Taken together, our data promote these two natural compound derivatives as potential promising anticancer compounds and provide breakthrough, novel findings on functional groups that can be used in drug development. Additionally, these results point out that the selective targeting of cancer cells can be reached and it is a reasonable aim during drug design and lead compound optimization. We think that the identification of cancer-specific molecules and pathways is one of the most desirable targets in cancer research and our data can open new horizons in this direction.

Abbreviations

aMan, α-Mangostin; aMan1, α-Mangostin-1; Pae, Paeonol; Pae1, Paeonol-1

Declarations

Ethics approval and consent to participate

The work was approved by the ethics committee of the Jena University Hospital with the approval 5032-01/17.

Consent for publication

All authors agreed for publication.

Competing interests

The authors declare no conflict of interest.

Availability of data and materials

All data are available from the Authors upon reasonable request.

Funding

This work was supported by funding from the Leibniz Institute on Aging (FLI), Alexander von Humboldt and Fritz-Thyssen foundation.

Authors' contributions

Designed experiments: SN, YPN, MR, KA, FA and FN. Performed experiments: SN, YPN, MR, KA, FN, LA, SK and FN. Developed and provided research reagents: YPH and MHH. Analyzed data: SN, YPN, MR, KA, FA,

MHH, and FN. Wrote the manuscript: SN, MR, KA, and FN.

Acknowledgements

The authors are grateful for the support by core facilities FACS, Sequencing and Microscopy at the Leibniz Institute on Aging – Fritz Lipmann Institute.

References

1 Hughes LAE, Simons C, van den Brandt PA, van Engeland M, Weijenberg MP. Lifestyle, Diet, and Colorectal Cancer Risk According to (Epi)genetic Instability: Current Evidence and Future Directions of Molecular Pathological Epidemiology. *Curr Colorectal Cancer Rep* 2017; 13: 455-469.

2 Araghi M, Soerjomataram I, Jenkins M, Brierley J, Morris E, Bray F *et al*. Global trends in colorectal cancer mortality: projections to the year 2035. *Int J Cancer* 2019; 144: 2992-3000.

3 Coppede F, Lopomo A, Spisni R, Migliore L. Genetic and epigenetic biomarkers for diagnosis, prognosis and treatment of colorectal cancer. *World J Gastroenterol* 2014; 20: 943-956.

4 Golshani G, Zhang Y. Advances in immunotherapy for colorectal cancer: a review. *Therap Adv Gastroenterol* 2020; 13: 1756284820917527.

5 Xie Y-H, Chen Y-X, Fang J-Y. Comprehensive review of targeted therapy for colorectal cancer. *Signal Transduction and Targeted Therapy* 2020; 5: 22.

6 Devlin EJ, Denson LA, Whitford HS. Cancer Treatment Side Effects: A Meta-analysis of the Relationship Between Response Expectancies and Experience. *J Pain Symptom Manage* 2017; 54: 245-258 e242.

7 Tofthagen C. Surviving chemotherapy for colon cancer and living with the consequences. *J Palliat Med* 2010; 13: 1389-1391.

8 Whitford HS, Olver IN. When expectations predict experience: the influence of psychological factors on chemotherapy toxicities. *J Pain Symptom Manage* 2012; 43: 1036-1050.

9 Newman DJ, Cragg GM. Natural products as sources of new drugs over the 30 years from 1981 to 2010. *J Nat Prod* 2012; 75: 311-335.

10 Nobili S, Lippi D, Witort E, Donnini M, Bausi L, Mini E *et al*. Natural compounds for cancer treatment and prevention. *Pharmacol Res* 2009; 59: 365-378.

11 Lee JH, Khor TO, Shu L, Su ZY, Fuentes F, Kong AN. Dietary phytochemicals and cancer prevention: Nrf2 signaling, epigenetics, and cell death mechanisms in blocking cancer initiation and progression. *Pharmacol Ther* 2013; 137: 153-171.

12 Zaidi SF, Ahmed K, Saeed SA, Khan U, Sugiyama T. Can Diet Modulate Helicobacter pylori-associated Gastric Pathogenesis? An Evidence-Based Analysis. *Nutr Cancer* 2017; 69: 979-989.

13 Abotaleb M, Samuel SM, Varghese E, Varghese S, Kubatka P, Liskova A *et al*. Flavonoids in Cancer and Apoptosis. *Cancers (Basel)* 2018; 11.

14 Saha S, Sadhukhan P, Sil PC. Mangiferin: A xanthonoid with multipotent anti-inflammatory potential. *Biofactors* 2016; 42: 459-474.

15 Shan T, Ma Q, Guo K, Liu J, Li W, Wang F *et al*. Xanthones from mangosteen extracts as natural chemopreventive agents: potential anticancer drugs. *Curr Mol Med* 2011; 11: 666-677.

16 Phan TKT, Shahbazzadeh F, Pham TTH, Kihara T. Alpha-mangostin inhibits the migration and invasion of A549 lung cancer cells. *PeerJ* 2018; 6: e5027.

17 Korm S, Jeong H-C, Kwon O-S, Park J-R, Cho H, Kim Y-M *et al*. α-Mangostin induces G1 cell cycle arrest in HCT116 cells through p38MAPK-p16INK4a pathway. *RSC Advances* (10.1039/C5RA00780A) 2015; 5: 34752-34760.

18 Martinez-Abundis E, Garcia N, Correa F, Hernandez-Resendiz S, Pedraza-Chaverri J, Zazueta C. Effects of alpha-mangostin on mitochondrial energetic metabolism. *Mitochondrion* 2010; 10: 151-157.

19 Xing G, Zhang Z, Liu J, Hu H, Sugiura N. Antitumor effect of extracts from moutan cortex on DLD-1 human colon cancer cells in vitro. *Mol Med Rep* 2010; 3: 57-61.

20 Zhang KJ, Gu QL, Yang K, Ming XJ, Wang JX. Anticarcinogenic Effects of alpha-Mangostin: A Review. *Planta Med* 2017; 83: 188-202.

21 Cai Y, Luo Q, Sun M, Corke H. Antioxidant activity and phenolic compounds of 112 traditional Chinese medicinal plants associated with anticancer. *Life Sci* 2004; 74: 2157-2184.

22 Li N, Fan LL, Sun GP, Wan XA, Wang ZG, Wu Q *et al*. Paeonol inhibits tumor growth in gastric cancer in vitro and in vivo. *World J Gastroenterol* 2010; 16: 4483-4490.

23 Lyu ZK, Li CL, Jin Y, Liu YZ, Zhang X, Zhang F *et al*. Paeonol exerts potential activities to inhibit the growth, migration and invasion of human gastric cancer BGC823 cells via downregulating MMP2 and MMP9. *Mol Med Rep* 2017; 16: 7513-7519.

24 Bao MH, Zhang YW, Zhou HH. Paeonol suppresses oxidized low-density lipoprotein induced endothelial cell apoptosis via activation of LOX-1/p38MAPK/NF-kappaB pathway. *J Ethnopharmacol* 2013; 146: 543-551.

25 Li M, Tan SY, Wang XF. Paeonol exerts an anticancer effect on human colorectal cancer cells through inhibition of PGE(2) synthesis and COX-2 expression. *Oncol Rep* 2014; 32: 2845-2853.

26 Kumar SK, Hager E, Pettit C, Gurulingappa H, Davidson NE, Khan SR. Design, synthesis, and evaluation of novel boronic-chalcone derivatives as antitumor agents. *J Med Chem* 2003; 46: 2813-2815.

27 Das BC, Thapa P, Karki R, Schinke C, Das S, Kambhampati S *et al*. Boron chemicals in diagnosis and therapeutics. *Future Med Chem* 2013; 5: 653-676.

28 Trippier PC, McGuigan C. Boronic acids in medicinal chemistry: anticancer, antibacterial and antiviral applications. *MedChemComm* (10.1039/C0MD00119H) 2010; 1: 183-198.

29 Thyss R, Virolle V, Imbert V, Peyron JF, Aberdam D, Virolle T. NF-kappaB/Egr-1/Gadd45 are sequentially activated upon UVB irradiation to mediate epidermal cell death. *EMBO J* 2005; 24: 128-137.

30 Mircetic J, Dietrich A, Paszkowski-Rogacz M, Krause M, Buchholz F. Development of a genetic sensor that eliminates p53 deficient cells. *Nat Commun* 2017; 8: 1463.

31 Boone DN, Qi Y, Li Z, Hann SR. Egr1 mediates p53-independent c-Myc-induced apoptosis via a noncanonical ARF-dependent transcriptional mechanism. *Proc Natl Acad Sci U S A* 2011; 108: 632-637.

32 Fellner C. Promising Drugs in Clinical Development To Treat Advanced Colorectal Cancer. *P T* 2017; 42: 262-265.

33 Sato T, Stange DE, Ferrante M, Vries RG, Van Es JH, Van den Brink S *et al*. Long-term expansion of epithelial organoids from human colon, adenoma, adenocarcinoma, and Barrett's epithelium. *Gastroenterology* 2011; 141: 1762-1772.

34 Grabinger T, Luks L, Kostadinova F, Zimberlin C, Medema JP, Leist M *et al*. Ex vivo culture of intestinal crypt organoids as a model system for assessing cell death induction in intestinal epithelial cells and enteropathy. *Cell Death Dis* 2014; 5: e1228.

35 Trapnell C, Roberts A, Goff L, Pertea G, Kim D, Kelley DR *et al*. Differential gene and transcript expression analysis of RNA-seq experiments with TopHat and Cufflinks. *Nat Protoc* 2012; 7: 562-578.

36 Anders S, Pyl PT, Huber W. HTSeq–a Python framework to work with high-throughput sequencing data. *Bioinformatics* 2015; 31: 166-169.

37 Love MI, Huber W, Anders S. Moderated estimation of fold change and dispersion for RNA-seq data with DESeq2. *Genome Biol* 2014; 15: 550.

38 Kramer A, Green J, Pollard J, Jr., Tugendreich S. Causal analysis approaches in Ingenuity Pathway Analysis. *Bioinformatics* 2014; 30: 523-530.

Figures

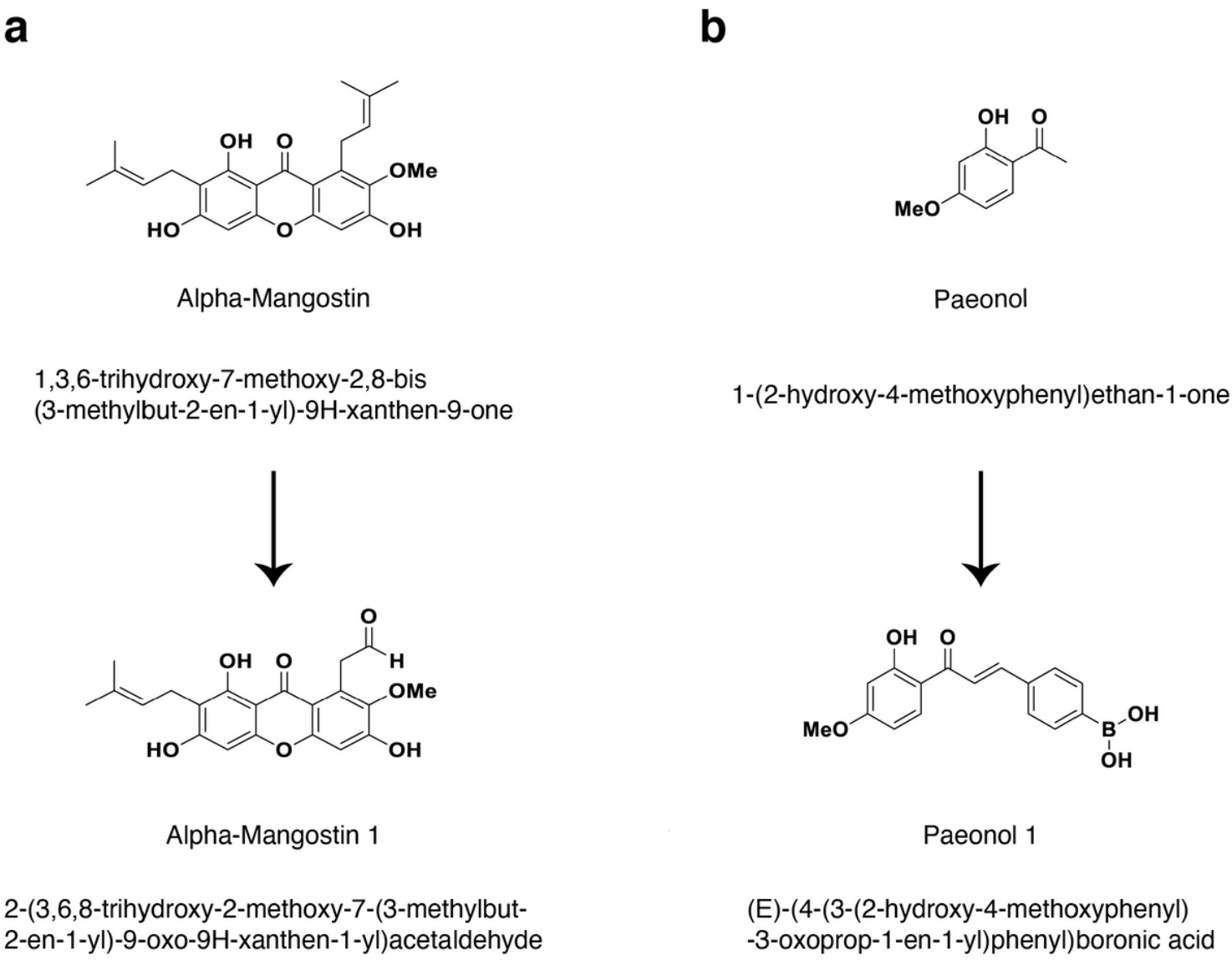

Figure 1

The chemical structure of natural compounds. (a) The structure of aMan and aMan1. (b) The structure of Pae and Pae1

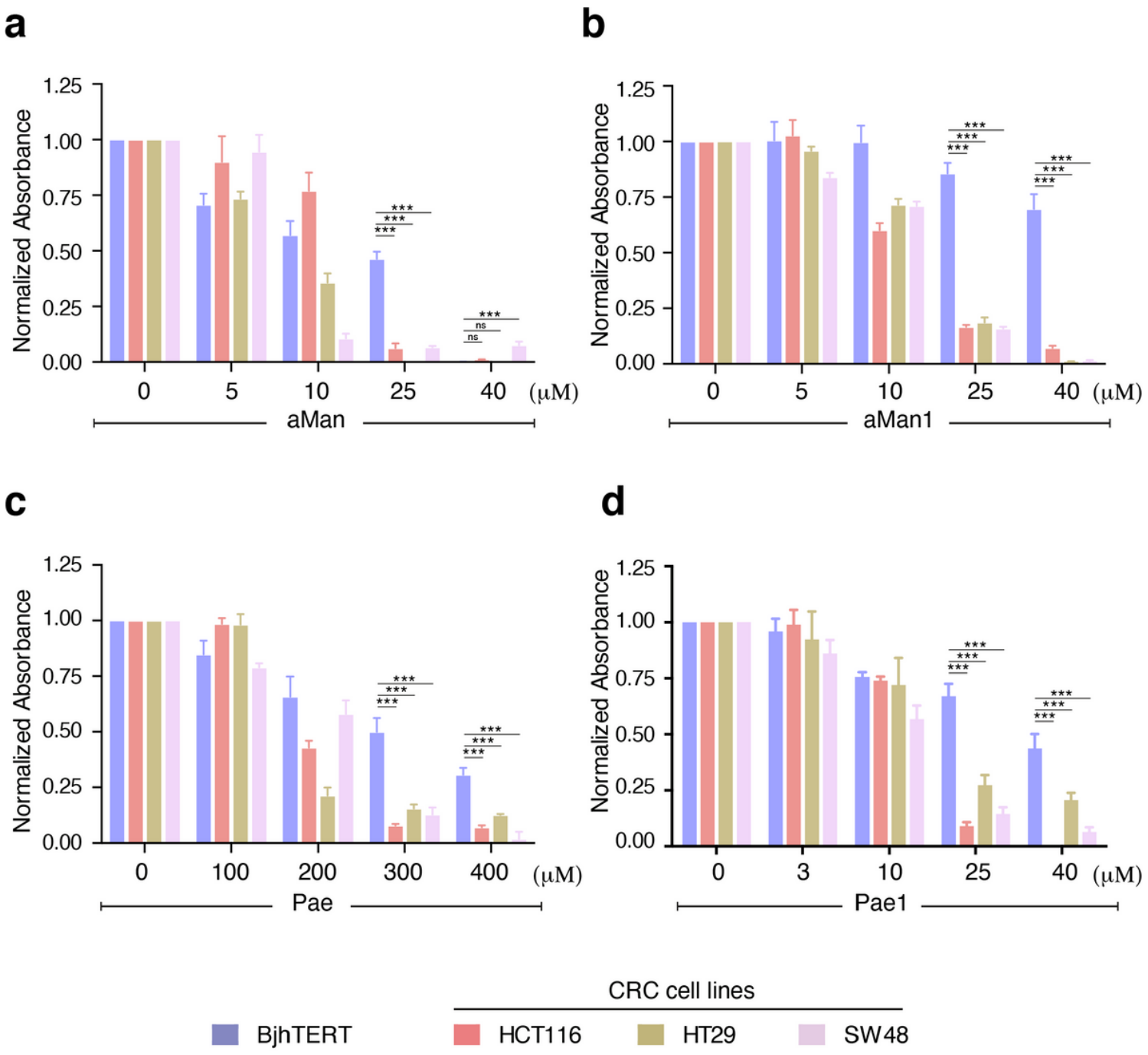

Figure 2

Natural compounds inhibit the growth of human colon cancer cells. aMan (5, 10, 25, and 40 μM) (a), aMan1 (5, 10, 25, and 40 μM) (b), Pae (100, 200, 300, and 400 μM) (c), or Pae1 (3, 10, 25, and 40 μM) (d) was added to BjhTERT, HCT116, HT-29, and SW48 cells at indicated concentrations for 72 h. The viability of the cells was quantified by crystal violet assay. Panels a, b, c, and d represent three independent experiments. The statistical significance between two groups were analysed by a two-tail unpaired T-test *P≤0.05, ** P≤0.01, and *** P≤0.001.

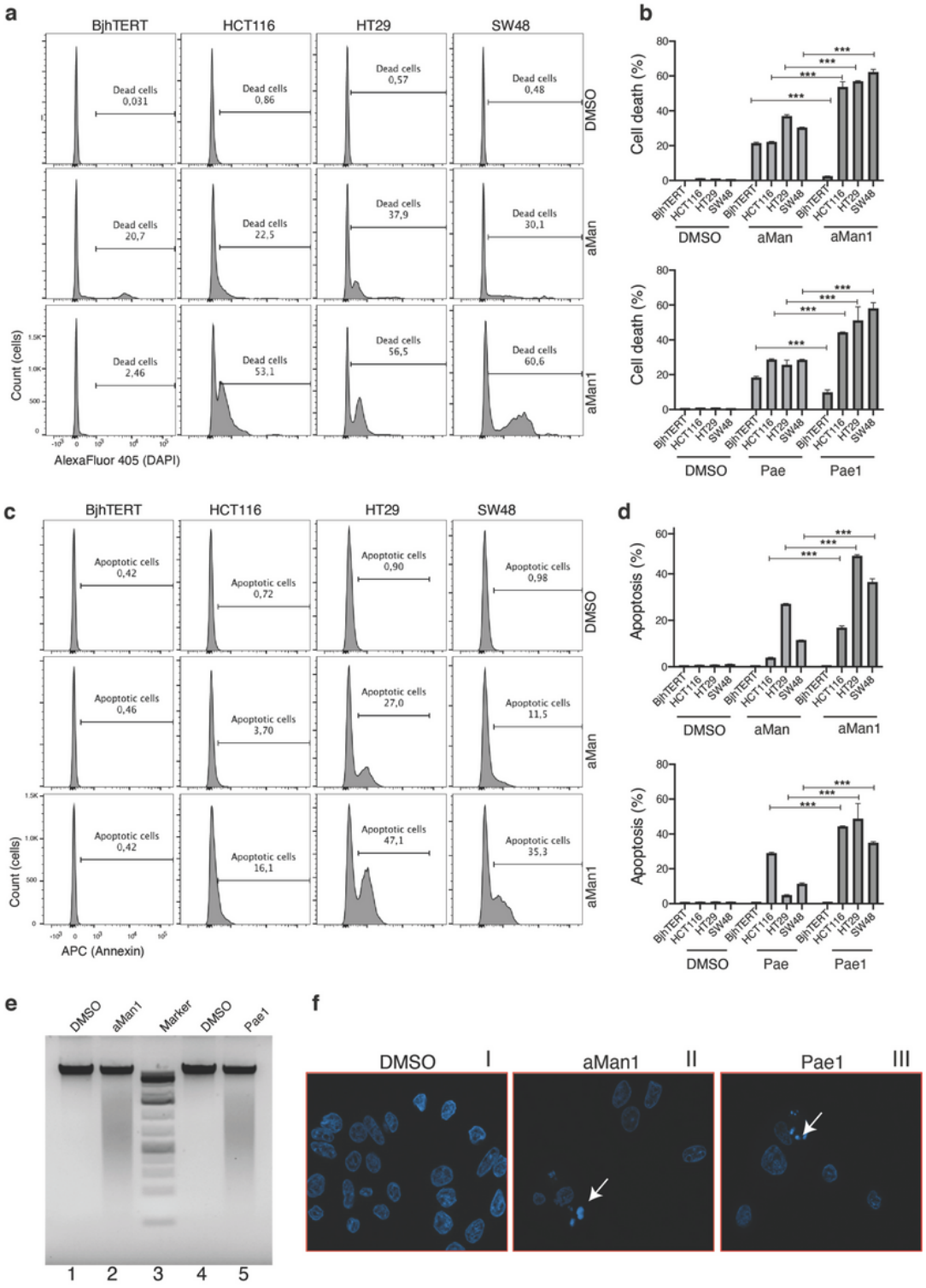

Figure 3

Natural compounds induce cell death, apoptosis, and DNA fragmentation in colon cancer cell lines. (a) aMan (25 μM) or aMan1 (25 μM) was added to BjhTERT, HCT116, HT-29, and SW48 cell lines. After 48 h, the cells were stained with DAPI, and the dead cells were quantified by flow cytometry. (b) Quantification of the dead cells (in percentage) in the indicated different cell lines with the indicated treatments. (n = 3). Pae and Pae1 were used at 300 μM and 10 μM, respectively. (c) Cells were treated as in (a) were stained

with Annexin V to quantify cell apoptosis by flow cytometry. (d) Quantification of the apoptotic cells (in percentage) in the indicated different cell lines with the indicated treatments. (n = 3). Pae was used at 300 μM, and Pae1 was used at 10 μM. aMan1 (25 μM) and Pae1 (10 μM) was incubated with SW48 cell lines. After 72 h, chromatin decondensation was visualized by agarose gel electrophoresis (e lanes 3 and 5) and confocal microscopy (f) as chromatin decondensation indicated by white arrows panel II and III) (f). Panels a, c, e, and f show single experiments from three independent replicates. Panels b and e indicate mean ± SD of three independent experiments. The significance between two groups were analysed by a two-tail unpaired T-test. *P≤0.05, ** P≤0.01, and *** P≤0.001.

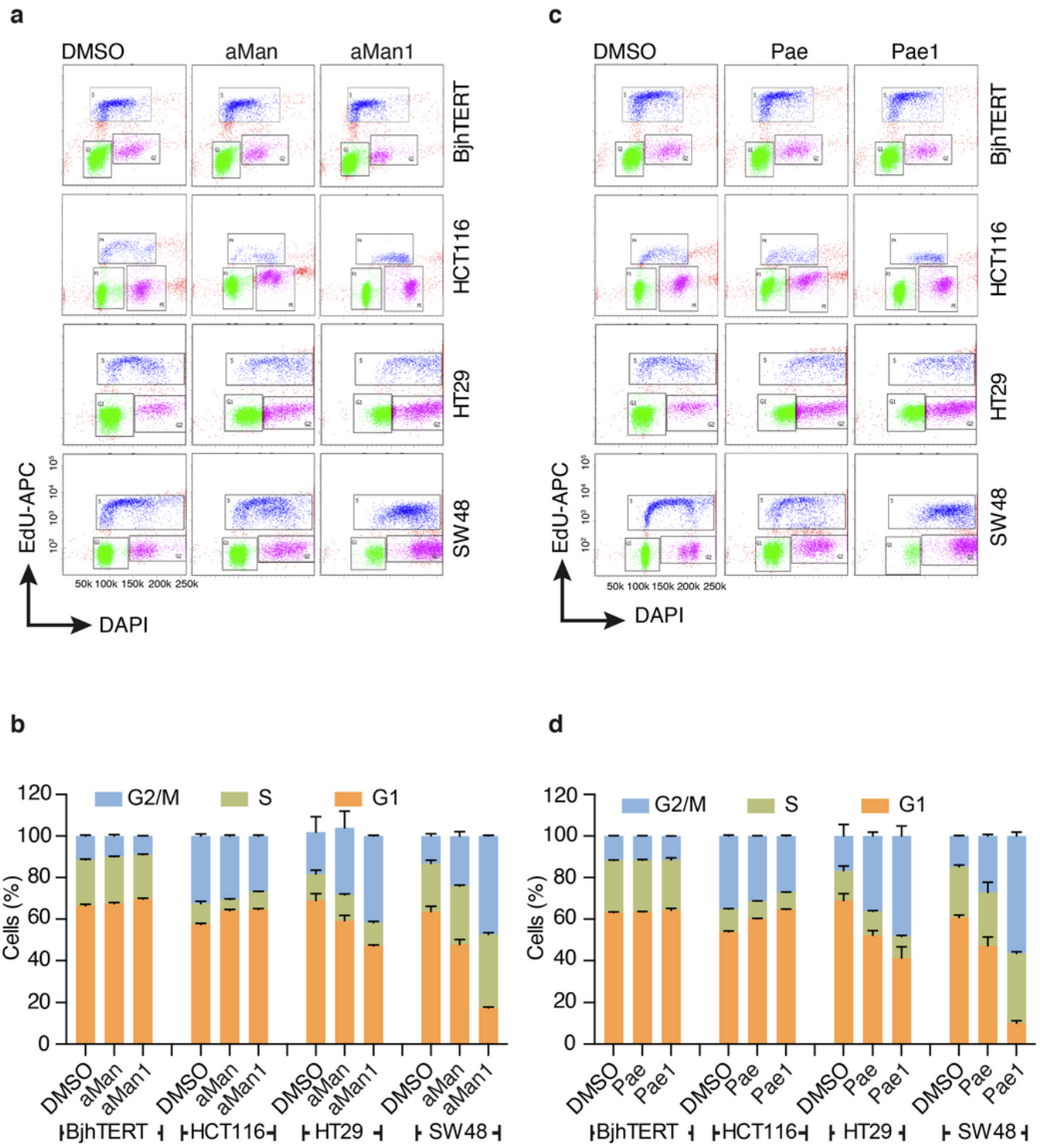

Figure 4

Natural compounds arrest colon cancer cell lines at G0 or G/M stage of cell cycle. (a) aMan (25 μM) or aMan1 (25 μM), or (c) Pae (300 μM), or Pae1 (10 μM) was added to BjhTERT, HCT116, HT-29, and SW48 cell lines for 48 h. Then the cells were incubated with 5-ethynyl-2´-deoxyuridine (EdU), a nucleoside analogue of thymidine that incorporates into DNA during active DNA synthesis. After incubation, the cells were stained with azide conjugated to Alexa Fluor® and DAPI and were analysed by FACS. (b, d)

Quantification of the distribution in each cell phase of cells treated with the indicated compounds. DMSO was used as control vehicle. Panel a and c indicate single experiments from two independent replicates. Panels b and d represent mean ± SD of two independent experiments.

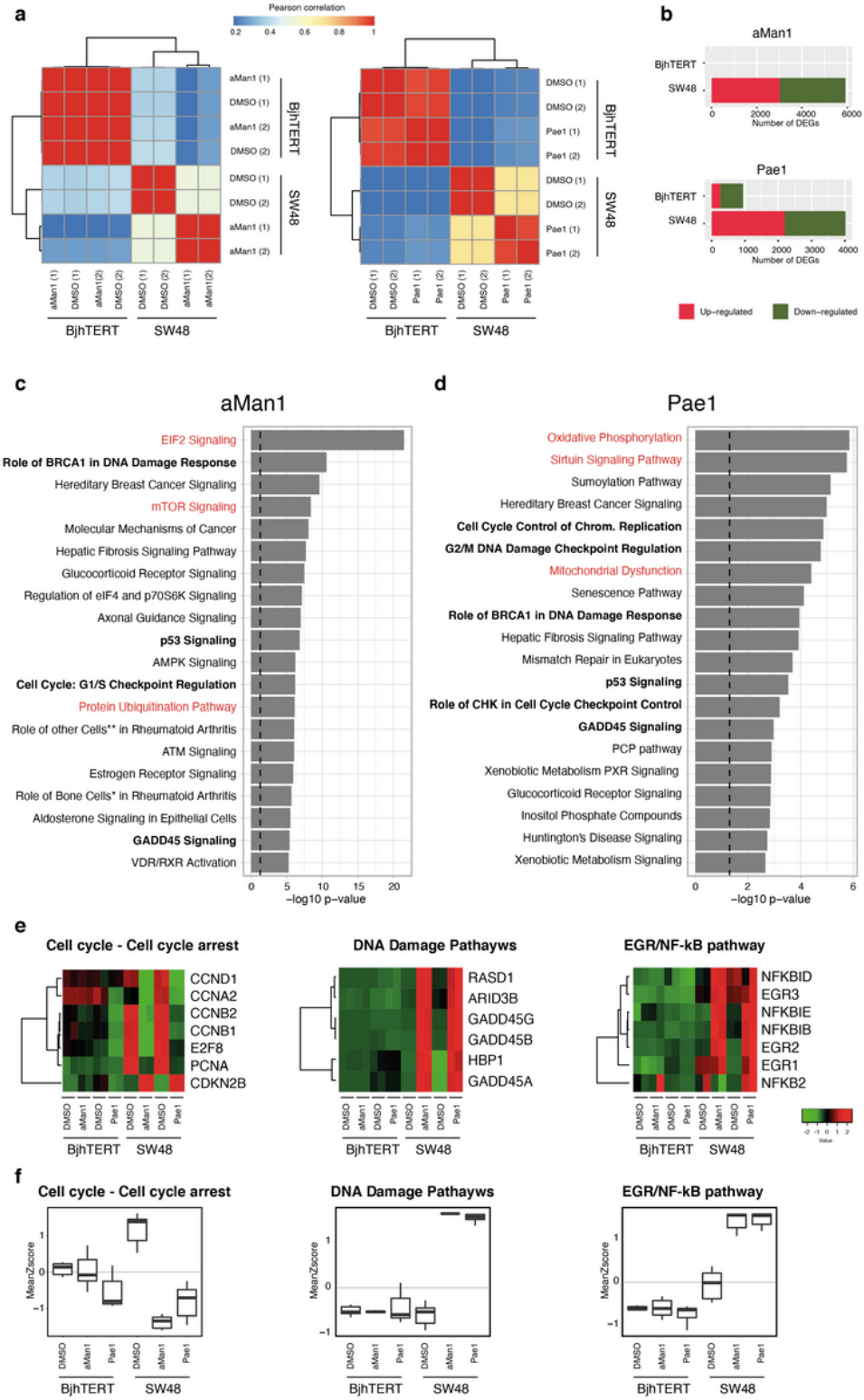

Figure 5

(a) aMan1 and Pae1 induce differentially expressed genes in SW48 CRC cell lines. Person correlation and hierarchical clustering of transcriptional profiles (RNA sequencing) of aMan1 (25 μM), Pae1 (10 μM) or

DMSO treated (24h) SW48 or BjhTERT cells. (b) Number of differentially expressed genes (DEGs) (adjusted p-value<0.05 & |log2 fold change|>=1) upon aMan1 or Pae1 treatment in the indicated cell lines. (c, d) Top 20 significantly enriched canonical pathways (IPA software) in DEGs (adjusted p-value<0.01 & |log2 fold change|>=1) found in SW48 cells upon aMan1(c), or Pae1 (d) treatment. The x axis shows the – log10 of enrichment p-value. The dashed line shows the statistical significance threshold (-log10 0.05=1.3). **Macrophages, Fibroblasts and Endothelial Cells, *Osteoblasts, Osteoclasts and Chondrocytes (e) Hierarchical clustering and heat map of 3 different gene set upon aMan1 or Pae1 treatment in the indicated cell lines. (f) Gene set enrichment analysis of the indicated gene sets (from e) in the specified conditions.

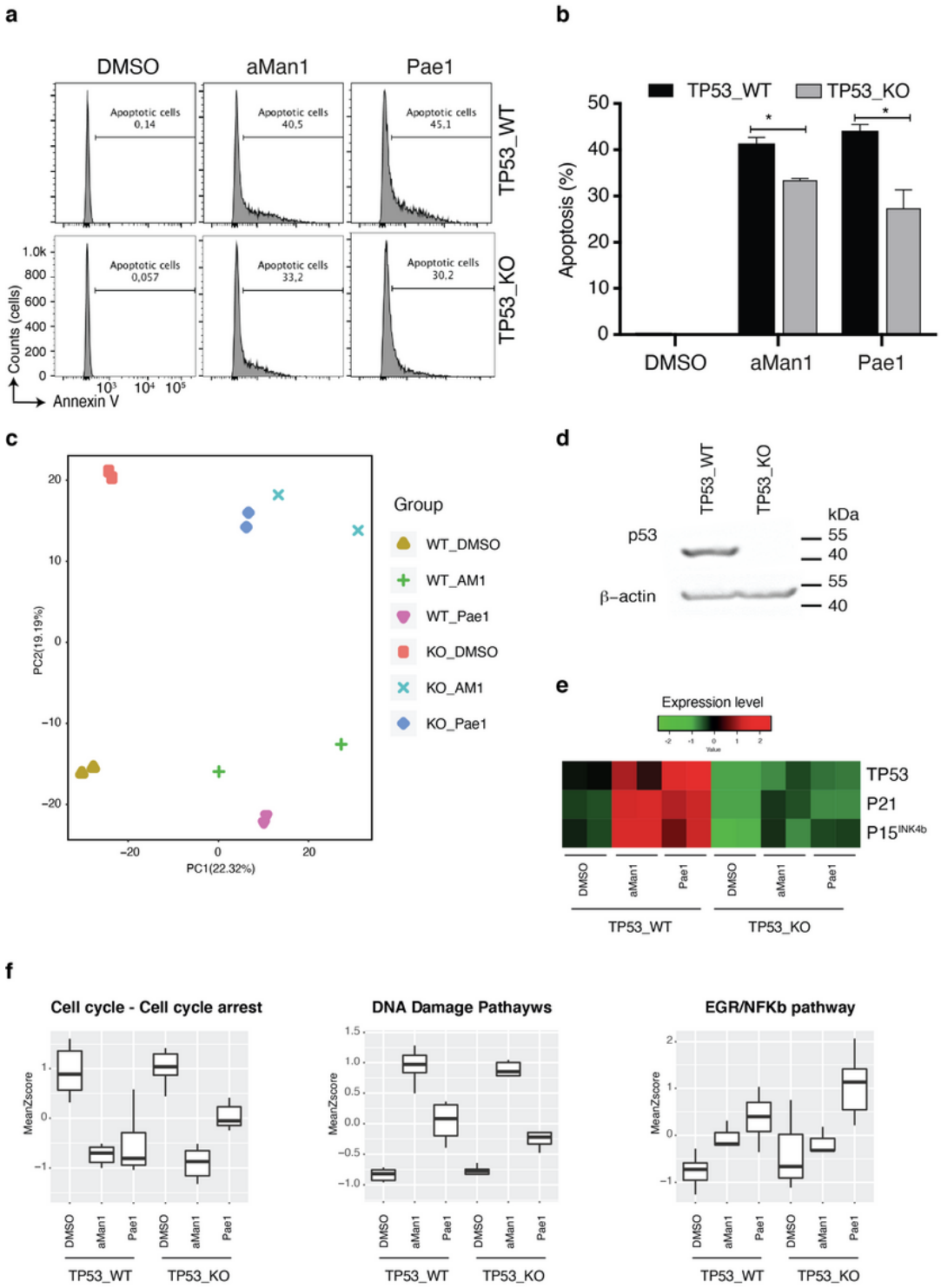

Figure 6

aMan1 and Pae1 induce higher percentage of apoptosis in HCT116 wild type cell than TP53 knockout cells. (a) aMan1 (25 μM) or and Pae1 (10 μM) was added to HCT116 wild type and TP53 knockout cells. After 48h, the cells were stained with Annexin V and analysed by flow cytometry. (b) Quantification of apoptosis (in percentage) in WT and KO cell lines with the indicated treatments. (c) Principal components analysis (PCA) of aMan1 or Pae1 treatment in HCT116 TP53_WT and TP53_KO cell lines. Expression of

p53 in HCT116 TP53_WT and TP53_KO was determined by Western blotting using p53 antibody (c upper panel), and b-actin served as a control (d lower panel). (e) Heat map of TP53, P21, and P15INK4b expression in aMan1, Pae1 or DMSO treated SW48 or BjhTERT cells. (F) Gene set enrichment analysis of the indicated gene sets (form 5E) in HCT116 TP53_WT and TP53_KO cell lines treated with DMSO, aMan1 or Pae1. Panels a and d indicate single experiments from three independent replicates. Panel B represents mean ± SD of three independent experiments. The *P≤0.05, ** P≤0.01, and *** P≤0.001. The statistical significance between two groups were analysed by a two-tail unpaired T-test.

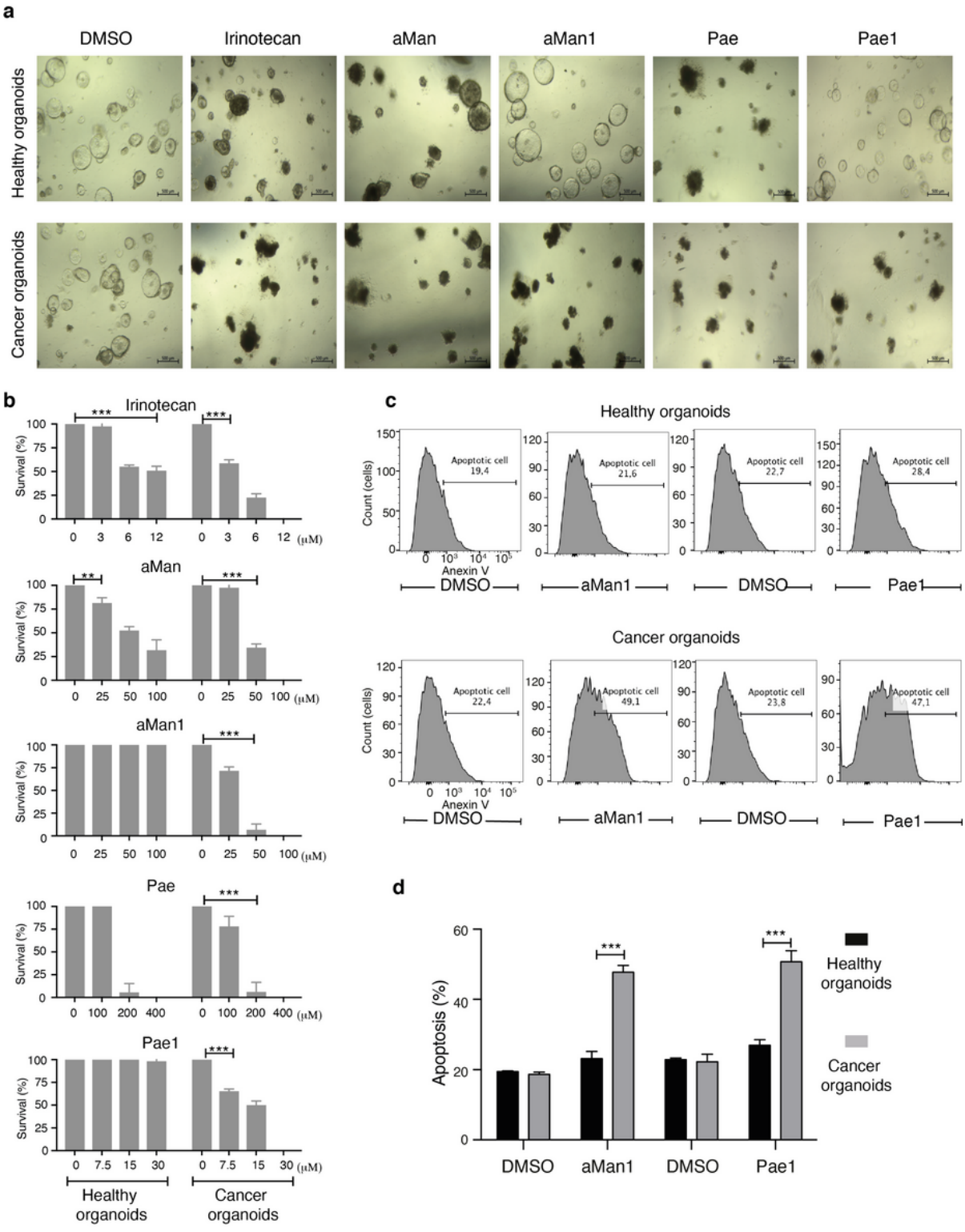

Figure 7

aMan1 and Pae1 induce cell death and apoptosis in human organoids derived from CRC, but not from healthy colon tissue. Irinotecan (3, 6, and, 12 μM) aMan (25, 50, and 100 μM), aMan1 (25, 50, and 100 μM), Pae1 (100, 200, and 400 μM), or Pae1 (7.5, 15, and 30 μM) was added to organoids derived from healthy colon epithelium (upper panel) or cancer tissue (lower panel) of the same patient (a). After 48 h of incubation, images of the organoids were captured. Quantification of the survival of organoids (in percentage) derived from healthy or tumor tissue treated with natural compounds (b). Natural compounds induced apoptosis was determined by flow cytometry annexin V staining (c). Quantification of the apoptotic cells (in percentage) in healthy and tumor organoid cells treated with aMan1 and Pae1 (n = 3) (d). Panel a, and c show single experiments out of three independent replicates. Panels b and d show mean ± SD of three independent experiments. *P≤0.05, ** P≤0.01, and *** P≤0.001. The statistical significance between two groups were analysed by a two-tail unpaired T-test.

Supplementary Files

This is a list of supplementary files associated with this preprint. Click to download.

- FigS1.png
- FigS2.png
- FigS3.png
- FigS4.png
- FigS5.png
- FigS6.png